Journal of Physics A: Mathematical and Theoretical



PAPER

OPEN ACCESS

RECEIVED
11 May 2026

REVISED
4 August 2026

ACCEPTED FOR PUBLICATION
13 August 2026

PUBLISHED
26 August 2026



# Electric field effects on the ionic relaxation in a finite slab adsorbing cell

A M Scarfone[1,2,4,*], G Barbero[1,2] and L R Evangelista[1,3,5]

[1] Istituto dei Sistemi Complessi del Consiglio Nazionale delle Ricerche (ISC-CNR) c/o Politecnico di Torino, Corso Duca degli Abruzzi 24, Torino 10129, Italy
[2] Dipartimento di Scienza Applicata e Tecnologia, Politecnico di Torino, Corso Duca degli Abruzzi 24, Torino 10129, Italy
[3] Departamento de Física, Universidade Estadual de Maringá, Avenida Colombo, Maringá 5790-87020-900, Paraná, Brazil
[4] Istituto Nazionale di Fisica Nucleare (INFN) — Sezione di Torino, 10125 Torino, Italy
[5] Dipartimento di Scienza Molecolare e Nanosistemi, Universitá di Venezia Ca' Foscari, Via Torino 155, Venezia 30175, Italy
[*] Author to whom any correspondence should be addressed.

**E-mail:** antoniomaria.scarfone@cnr.it

**Keywords:** Poisson–Nernst–Planck model, Langmuir kinetic equation, adsorption–desorption phenomena, charge and discharge processes

## Abstract

This paper is a natural continuation of the study done in Scarfone *et al* (2026 Electric field effects on the ionic relaxation in a semi-infinite adsorbing cell *J. Phys. A: Math. Theor.* **59** 205201). We analyze the distribution of mobile charges for a slab geometry with well-defined thickness under selectively adsorbing surfaces. For simplicity, only positive charges are considered mobile. The full scenario is characterized by bulk drift and diffusion, together with selective charge adsorption at the surfaces. The problem is addressed within the Poisson–Nernst–Planck model framework, in which the continuity equation for the mobile charges is coupled to Poisson's equation, while the Langmuir balance equation governs selective adsorption at the surface. The time evolution of the system in the presence of an external power supply, as well as the dependence of the longest relaxation time on the applied potential difference, are also analyzed.

## 1. Introduction

We study the general problem of selective adsorption of positive charges on the limiting surfaces of typical electrolytic cells with a finite sample, bounded by two homogeneous planar-parallel adsorbing surfaces at a distance $d$ apart, placed at $z = \pm d/2$ of an orthogonal Cartesian system. In this framework, the bulk density of adsorbable particles depends only on the distance of the point considered from the limiting surfaces. Therefore, this geometry allows us to treat the mathematical problem as a one-dimensional spatial problem. It is known as slab geometry. In addition, we consider a time-dependent electric field, $\boldsymbol{E}$, which may or may not be applied to the sample along the $z$-direction.

Although expressed in simple terms, these theoretical scenarios can represent important practical problems in a variety of physical settings. Indeed, this model is widely used to analyze experimental data obtained by impedance spectroscopy [1, 2], and it has been generalized to account for anomalous diffusion and reaction terms in the medium [3, 4]. The simplest problem of a semi-infinite sample, with a limiting flat surface placed at the origin of a Cartesian reference frame, has been investigated in the companion paper [5].

The model is based on the ion continuity equation, namely the drift-diffusive Fokker–Planck equation and the Poisson equation for the electric field generated by the charge density [6]. This framework is consistent with the classical theory of electrochemical systems and diffuse charge dynamics [7–10], and it is related to more general descriptions of interfacial charge structure in confined electrolytes [11]. For simplicity, we assume that only positive ions are mobile and that diffusion is described by Fick's law. This scenario has been considered by several authors in view of its practical importance [12–15]. The model for this physical situation may be particularly useful for systems in which

salt is dissolved in a hydrogel, where large ions cannot move across the gel matrix or are trapped on the matrix by means of electrostatic interaction, as discussed in [16]. Further, we assume that, in the absence of adsorption, the medium is globally and locally neutral, and $n_0$ denotes the bulk density of positive and negative ions.

In this situation, the effective electric field, in the absence of an externally applied potential, is null across the sample. When adsorption at the surface takes place, the ions move towards the adsorbing surface and give rise to a particle current density $\boldsymbol{j}(\boldsymbol{r},t)$, perturbing the ionic distribution of the mobile ions $n(\boldsymbol{r},t)$ around the point $\boldsymbol{r}$ at time $t$, together with the resulting electric field $\boldsymbol{E}(\boldsymbol{r},t)$. This also occurs to a greater extent in the case of an externally applied power supply.

In this section, we recall the main equations on which our theoretical analysis for the slab geometry is based, discussed in detail in [5] for a semi-infinite sample.

We assume the continuity equation for the mobile ions, given by

$$\frac{\partial n}{\partial t} = -\boldsymbol{\nabla}\cdot\boldsymbol{j}, \tag{1.1}$$

where the current density, $\boldsymbol{j}(\boldsymbol{r},t)$, for neutral particles, is

$$\boldsymbol{j}(\boldsymbol{r},t) = -D\,\boldsymbol{\nabla}\,n(\boldsymbol{r},t), \tag{1.2}$$

with $D$ being the diffusion coefficient in the considered matrix. In the presence of an electric field $\boldsymbol{E}$, either external or induced by the adsorbed charged particles, the current density becomes

$$\boldsymbol{j}(\boldsymbol{r},t) = -D\left(\boldsymbol{\nabla}\,n(\boldsymbol{r},t) - \frac{q}{k_{\mathrm{B}}T}\,n(\boldsymbol{r},t)\,\boldsymbol{E}(\boldsymbol{r},t)\right), \tag{1.3}$$

where $q$ is the electric charge of the ion, $k_{\mathrm{B}}$ is the Boltzmann constant, and $T$ is the absolute temperature. Equation (1.3) is the current part of the so-called Nernst–Planck equation, which describes the influence of a concentration gradient and of the electric field on the flux of the charge carriers, usually ions [17, 18]. The current entering this equation usually involves three key processes: diffusion, migration (due to an electric field), and convection, which is not considered here.

The electric field is related to the particle density by means of the Poisson equation

$$\boldsymbol{\nabla}\cdot\boldsymbol{E} = \frac{q}{\varepsilon}\,(n - n_0), \tag{1.4}$$

with $\varepsilon$ representing the dielectric constant of the medium in which the ions are dispersed. This description is consistent with the classical theory of electrostatic screening and diffuse charge layers developed by Gouy and Chapman [19].

The analysis must account for diffusion processes in the bulk and adsorption–desorption kinetics at the interfaces. Therefore, if we denote by $\sigma$ the surface density of the adsorbed particles, the boundary conditions relating the bulk and the surface densities are given by

$$\boldsymbol{j}\cdot\boldsymbol{u}_n = \frac{\mathrm{d}\sigma}{\mathrm{d}t} \quad \text{and} \quad \boldsymbol{E}\cdot\boldsymbol{u}_n = \frac{q}{\varepsilon}\,\sigma, \tag{1.5}$$

where $\boldsymbol{u}_n$ is the outward-directed unit vector normal to the limiting surface. The coupling between interfacial charge and electric field is consistent with classical descriptions of adsorption phenomena in electrochemical systems [20].

Armed with these conceptual tools, we will address the problem of ionic motion in a typical electrolytic cell of finite thickness in the presence of an electric field, seeking to obtain analytical solutions for the charge distribution in the bulk and at the surface, both in the transient regime and at equilibrium.

Although the present work is restricted to ionic transport in electrolytic cells within the Poisson–Nernst–Planck (PNP) framework, certain elements of the mathematical formalism developed here may prove useful in future extensions toward plasma–liquid discharge systems. Examples include discharges involving liquid electrodes, plasmas generated in liquid bubbles, and dielectric barrier discharges in contact with liquids, provided that additional physical mechanisms, such as plasma generation, ionization, recombination, charge injection, and sheath formation, are incorporated into the model [21–24].

Our goal is to obtain an analytical solution of the ionic relaxation in a liquid in the presence of adsorption. For this reason, we work in the same frame as in [5], where the fundamental equations of the problem can be linearized. This implies that we limit our considerations to small adsorption, in

which the surface density of adsorbed ions is very small with respect to the surface density of adsorption sites. Furthermore, the applied electric field is small, in such a manner that the relative bulk variation of the ionic density is small. Of course, large adsorption and large electric field, responsible for large variations of the bulk density of ions, are important extensions of the problem. However, they require a numerical solution of the problem, and in particular a generalization of the kinetic equation describing the adsorption. These generalizations are beyond the aim of our paper.

The paper is organized as follows. In section 2, we present the mathematical problem of the slab in its simplest version, formulated by means of the fundamental equations and the relevant boundary conditions. In section 3, we separate the problem into equilibrium and transient components, analyzing the equilibrium configuration and the transient behavior and presenting the analytical solution of our problem. In section 4 we analyze the relaxation time for this problem. In section 5, we extend the study to the evolution of the system toward equilibrium in the presence of an external power supply that fixes the difference in electric potential between the electrodes. In section 6, we study the electric current inside the cell arising when the external potential is turned on. In section 7, we extend the study of the relaxation time in the presence of an external generator. In section 8 the merits and limits of our analysis are critically analyzed. Section 9 is devoted to the conclusions, whilst in appendices A and B we detail the analytical derivation of our solutions.

## 2. The PNP model for the slab

We consider a sample in the shape of a slab of thickness $d$, and introduce a Cartesian reference frame with the origin at the left side of the sample. In this framework, $-d/2 \leqslant z \leqslant d/2$. We assume that the adsorption phenomenon at the electrodes is well described by Langmuir's kinetic equation, in which the evolution of the surface density of adsorbed particles is given by

$$\frac{\mathrm{d}}{\mathrm{d}t}\sigma(t) = \kappa_a\, n(z,t)\Big|_{z=\mp d/2} - \frac{1}{\tau_a}\,\sigma(t), \tag{2.1}$$

where $\kappa_a$ and $\tau_a$ are phenomenological parameters connected with the adsorption coefficient and the desorption time, respectively. For simplicity, we assume that the two surfaces have the same physicochemical properties. Note also that equation (2.1) is valid in the limit of weak adsorption, i.e., for $\sigma$ very small with respect to the density of adsorption sites [25]. Indeed, equation (2.1) corresponds to the low-coverage limit of Langmuir adsorption kinetics, valid for $\sigma \ll \sigma_{\max}$, where $\sigma_{\max}$ denotes the density of available surface adsorption sites. Consequently, the present theory is restricted to weak adsorption, small concentration perturbations, and moderate applied voltages, while nonlinear effects such as site saturation, steric crowding, and Stern-layer corrections lie beyond the scope of the present analysis. In [26], finite-size and steric effects are discussed, pointing also to the limitations of classical dilute-solution description as well as the motivations for nonlinear interfacial models. Nonlinear adsorption kinetics are discussed in the classic paper by Langmuir [27] and, more recently, in [28], in which the approach combines adsorption with electrochemical interfaces. The work of Langmuir justifies the finite-capacity adsorption law, while in [28] we can find support for the idea that steric and nonlinear interfacial effects become important at high voltages.

As in [5], we use dimensionless space and time coordinates defined in $z \to \zeta = z/\Lambda$ and $t \to \tau = t/\tau_0$, with

$$\Lambda = \sqrt{\frac{\varepsilon\, k_{\mathrm{B}}\, T}{n_0\, q^2}}, \tag{2.2}$$

the Debye's length, and

$$\tau_0 = \frac{\Lambda^2}{D}, \tag{2.3}$$

the relaxation time. Consequently $-M \leqslant \zeta \leqslant M$, where $M = d/(2\,\Lambda)$. We also introduce the dimensionless quantities $\mathcal{N} = n/n_0$, $\mathcal{S} = \sigma/(n_0\,\Lambda)$, and $\mathcal{E} = \Lambda\, E/V_{\mathrm{th}}$, where $V_{\mathrm{th}} = k_{\mathrm{B}}\, T/q$ is the thermal voltage.

In terms of dimensionless quantities, the fundamental equations of the problem, equations (1.3) and (1.4), in the linear approximation valid in the limit of weak adsorption, become [5]

$$\frac{\partial \mathcal{N}}{\partial \tau} = \frac{\partial^2 \mathcal{N}}{\partial \zeta^2} - \frac{\partial \mathcal{E}}{\partial \zeta}, \tag{2.4}$$

$$\frac{\partial \mathcal{E}}{\partial \zeta} = \mathcal{N} - 1, \tag{2.5}$$

together with the kinetic equation (2.1) at the interfaces, which, in terms of reduced quantities, can be rewritten as

$$\mathcal{N}(\zeta, \tau)\Big|_{\zeta = \mp M} = \frac{1}{a}\left(\frac{\partial}{\partial \tau} + \frac{1}{b}\right)\mathcal{S}^{\mathrm{L/R}}(\tau), \tag{2.6}$$

where $\mathcal{S}^{\mathrm{L/R}}(\tau)$ refers to the surface density of adsorbed particles on the left ($\zeta = -M$) and the right ($\zeta = M$) plate, respectively. We denote by $a = \kappa_a \tau_0/\Lambda$ the dimensionless adsorption coefficient and by $b = \tau_a/\tau_0$ the dimensionless adsorption time. As discussed in [5, 7, 29], the parameters $a$ and $b$ are in the range .1–10 using reasonable values of the adsorption energy and the range of the surface forces responsible for the adsorption phenomenon and for the diffusion coefficient, dielectric constant, and ionic density in the liquid [5]. From the definition of the dimensionless adsorption coefficient, it is evident that in this problem there is an intrinsic adsorption coefficient given by $\Lambda/\tau_0$.

Before proceeding, we underline that throughout this work, transport is assumed to occur solely by diffusion and electromigration. Convective and electroosmotic effects are neglected, so that the model is applicable to quiescent systems (e.g., solid or gel electrolytes, or liquid electrolytes where fluid motion is negligible) [7, 30]. Incorporating fluid flow would require coupling the PNP equations to the Navier–Stokes equations and is left for future investigation.

When the limiting surfaces are adiabatic with respect to the adsorption phenomenon, for $\tau < 0$ the system is at electrically neutral equilibrium, with $\mathcal{N}(\zeta) = 1$ and $\mathcal{E}(\zeta) = 0$ for all $-M \leqslant \zeta \leqslant M$, and $\mathcal{S}^{\mathrm{L/R}} = 0$. At $\tau = 0$ adsorption takes place. The system evolves toward a new equilibrium configuration characterized by $\mathcal{N}_{\mathrm{eq}}(\zeta) \neq 1$, $\mathcal{E}_{\mathrm{eq}}(\zeta) \neq 0$, and $\mathcal{S}^{\mathrm{L/R}}_{\mathrm{eq}} \neq 0$.

Let us observe that conservation of the number of particles implies

$$\mathcal{S}^{\mathrm{L}}(\tau) + \mathcal{S}^{\mathrm{R}}(\tau) + \int_{-M}^{M}\Big(\mathcal{N}(\zeta, \tau) - 1\Big)\,\mathrm{d}\zeta = 0, \tag{2.7}$$

since what is missing in the bulk is necessarily accumulated on the surfaces.

By differentiating this relation with respect to $\tau$ and taking into account equation (2.4), we get

$$\frac{\mathrm{d}}{\mathrm{d}\tau}\mathcal{S}^{\mathrm{L/R}}(\tau) = \pm\left(\frac{\partial \mathcal{N}}{\partial \zeta} - \mathcal{E}\right)_{\zeta = \mp M}, \tag{2.8}$$

which are boundary conditions that must be satisfied at the sample surfaces. In addition, we have

$$\mathcal{S}^{\mathrm{L}}(\tau) = \mathcal{E}(-M, \tau) = -\mathcal{E}(M, \tau) = \mathcal{S}^{\mathrm{R}}(\tau), \tag{2.9}$$

which are consequences of Coulomb's theorem, which states that the surface electric field is proportional to the surface charge density.

The electric field, given by equation (2.5), changes from the initial configuration $\mathcal{E}(\zeta, 0) = 0$ to

$$\begin{aligned}\mathcal{E}(\zeta, \tau) &= \mathcal{E}(-M, \tau) + \int_{-M}^{\zeta}\Big(\mathcal{N}(\eta, \tau) - 1\Big)\,\mathrm{d}\eta \\ &= \mathcal{E}(M, \tau) - \int_{\zeta}^{M}\Big(\mathcal{N}(\eta, \tau) - 1\Big)\,\mathrm{d}\eta.\end{aligned} \tag{2.10}$$

Actually, when no external electric potential is applied, $\mathcal{N}(\zeta, \tau)$ is the fundamental quantity of our problem. It is the solution of the partial differential equation

$$\frac{\partial \mathcal{N}}{\partial \tau} = \frac{\partial^2 \mathcal{N}}{\partial \zeta^2} - (\mathcal{N} - 1), \tag{2.11}$$

obtained by combining equations (2.4) and (2.5). It is a generalized diffusion equation with an internal source term.

When adsorption takes place, the system evolves toward a new equilibrium configuration $\mathcal{N}(\zeta, \infty) \equiv \mathcal{N}_{\mathrm{eq}}(\zeta)$, whose solution must satisfy the initial condition $\mathcal{N}(\zeta, 0) = 1$. The kinetics, governed by equation (2.11), is constrained by equation (2.6). Once the solution $\mathcal{N}(\zeta, \tau)$ is known, the surface density of adsorbed particles $\mathcal{S}^{\mathrm{L/R}}(\tau)$ follows from equation (2.7), since by symmetry $\mathcal{S}^{\mathrm{L}}(\tau) = \mathcal{S}^{\mathrm{R}}(\tau)$, while the electric field $\mathcal{E}(\zeta, \tau)$ follows from equation (2.10).

## 3. Equilibrium and transient solutions

We look for a solution to the problem, separated into an equilibrium and transient components, according to

$$\mathcal{N}(\zeta,\tau)=\mathcal{N}_{\rm eq}(\zeta)+\mathcal{N}_{\rm tr}(\zeta,\tau), \tag{3.1}$$
$$\mathcal{E}(\zeta,\tau)=\mathcal{E}_{\rm eq}(\zeta)+\mathcal{E}_{\rm tr}(\zeta,\tau), \tag{3.2}$$
$$\mathcal{S}(\tau)=\mathcal{S}_{\rm eq}+\mathcal{S}_{\rm tr}(\tau). \tag{3.3}$$

From the system of equations (2.4)–(2.6), we have

$$\frac{\partial^2}{\partial\zeta^2}\mathcal{N}_{\rm eq}(\zeta)-\frac{\partial}{\partial\zeta}\mathcal{E}_{\rm eq}(\zeta)=0, \tag{3.4}$$
$$\frac{\partial}{\partial\zeta}\mathcal{E}_{\rm eq}(\zeta)=\mathcal{N}_{\rm eq}(\zeta)-1, \tag{3.5}$$
$$\mathcal{S}_{\rm eq}^{\rm L}=ab\mathcal{N}_{\rm eq}(-M)=ab\mathcal{N}_{\rm eq}(M)=\mathcal{S}_{\rm eq}^{\rm R}, \tag{3.6}$$

for the equilibrium components, and

$$\frac{\partial}{\partial\tau}\mathcal{N}_{\rm tr}(\zeta,\tau)=\frac{\partial^2}{\partial\zeta^2}\mathcal{N}_{\rm tr}(\zeta,\tau)-\frac{\partial}{\partial\zeta}\mathcal{E}_{\rm tr}(\zeta,\tau), \tag{3.7}$$
$$\frac{\partial}{\partial\zeta}\mathcal{E}_{\rm tr}(\zeta,\tau)=\mathcal{N}_{\rm tr}(\zeta,\tau), \tag{3.8}$$
$$\mathcal{N}_{\rm tr}(\zeta,\tau)\Big|_{\zeta=\mp M}=\frac{1}{a}\left(\frac{\partial}{\partial\tau}+\frac{1}{b}\right)\mathcal{S}_{\rm tr}(\tau), \tag{3.9}$$

for the transient components, where $\mathcal{S}_{\rm tr}^{\rm L}(\tau)=\mathcal{S}_{\rm tr}^{\rm R}(\tau)\equiv\mathcal{S}_{\rm tr}(\tau)$ and

$$\mathcal{S}_{\rm tr}(\tau)+\frac{1}{2}\int_{-M}^{M}\mathcal{N}_{\rm tr}(\zeta,\tau)\,{\rm d}\zeta=0. \tag{3.10}$$

Accounting for equation (2.9), the solutions for the equilibrium components read

$$\mathcal{N}_{\rm eq}(\zeta)=1-\frac{ab\cosh(\zeta)}{\sinh(M)+ab\cosh(M)}, \tag{3.11}$$
$$\mathcal{E}_{\rm eq}(\zeta)=-\frac{ab\sinh(\zeta)}{\sinh(M)+ab\cosh(M)}, \tag{3.12}$$
$$\mathcal{S}_{\rm eq}=\frac{ab}{1+ab\coth(M)}. \tag{3.13}$$

In contrast, the transient components can be obtained starting from the solution of the equation

$$\frac{\partial\mathcal{N}_{\rm tr}}{\partial\tau}=\frac{\partial^2\mathcal{N}_{\rm tr}}{\partial\zeta^2}-\mathcal{N}_{\rm tr}, \tag{3.14}$$

subject to the initial condition

$$\mathcal{N}_{\rm tr}(\zeta,0)=1-\mathcal{N}_{\rm eq}(\zeta), \tag{3.15}$$

and the boundary condition

$$\mathcal{N}_{\rm tr}(-M,\tau)=\mathcal{N}_{\rm tr}(M,\tau)=-\frac{1}{2a}\int_{-M}^{M}\left(\frac{\partial}{\partial\tau}+\frac{1}{b}\right)\mathcal{N}_{\rm tr}(\zeta,\tau)\,{\rm d}\zeta, \tag{3.16}$$

as follows from combining equations (2.6) and (2.7) for the transient component. In addition, $\mathcal{N}_{\rm tr}(\zeta,\tau)$ must vanish in the $\tau\to\infty$ limit, i.e. $\mathcal{N}_{\rm tr}(\zeta,\infty)=0$, to ensure that in the same limit $\mathcal{N}\to\mathcal{N}_{\rm eq}$.

Boundary conditions on $\mathcal{N}_{\rm tr}(\zeta,\tau)$ induce analogous conditions on $\mathcal{E}_{\rm tr}(\zeta,\tau)$ and $\mathcal{S}_{\rm tr}(\tau)$, given, respectively, by

$$\mathcal{E}_{\rm tr}(\zeta,\infty)=0,\quad\text{and}\quad\mathcal{E}_{\rm tr}(\zeta,0)=-\mathcal{E}_{\rm eq}(\zeta), \tag{3.17}$$
$$\mathcal{S}_{\rm tr}(\infty)=0,\quad\text{and}\quad\mathcal{S}_{\rm tr}(0)=-\mathcal{S}_{\rm eq}. \tag{3.18}$$

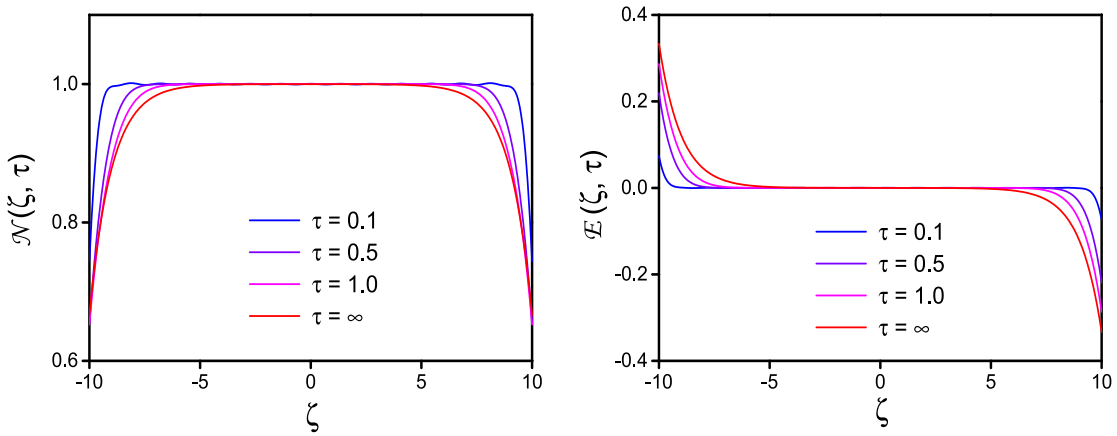


**Figure 1.** Left panel: shape of $\mathcal{N}(\zeta,\tau)$ vs $\zeta$, approaching the equilibrium configuration (red line) (cfr. equation (3.11)), depicted for several values of $\tau$. The initial distribution, given by $\mathcal{N}(\zeta,0)=1$ is not reported. Right panel: shape of $\mathcal{E}(\zeta,\tau)$ vs $\zeta$, approaching the equilibrium configuration (red line) (cfr. equation (3.12)), depicted for several values of $\tau$. The initial distribution, given by $\mathcal{E}(\zeta,0)=0$ is not reported. The curves are drawn for $a=1$, $b=0.5$, and $M=10$.

The analytical solution for the transient components is presented in appendix A, and is summarized hereinafter in

$$\mathcal{N}(\zeta,\tau)=1-\frac{ab\cosh(\zeta)}{\sinh(M)+ab\cosh(M)} - ab\sum_{k=1}^{\infty}\frac{\sqrt{1+p_k}\cosh\left(\zeta\sqrt{1+p_k}\right)}{G'(p_k)\,p_k\cosh\left(M\sqrt{1+p_k}\right)}\,\mathrm{e}^{p_k\tau}, \tag{3.19}$$

$$\mathcal{E}(\zeta,\tau)=\frac{ab}{1+ab\coth(M)} - ab\sum_{k=1}^{\infty}\frac{\sinh\left(\zeta\sqrt{1+p_k}\right)}{G'(p_k)\,p_k\cosh\left(M\sqrt{1+p_k}\right)}\,\mathrm{e}^{p_k\tau}, \tag{3.20}$$

$$\mathcal{S}(\tau)=\frac{ab}{1+ab\coth(M)} + ab\sum_{k=1}^{\infty}\frac{\tanh\left(M\sqrt{1+p_k}\right)}{G'(p_k)\,p_k}\,\mathrm{e}^{p_k\tau}, \tag{3.21}$$

with

$$G(p)=ab\sqrt{1+p}+(1+bp)\tanh\left(M\sqrt{1+p}\right), \tag{3.22}$$

where $p_k$ are the zeros of the function $G(p)$ (see appendix A).

The shape of the bulk density of particles $\mathcal{N}(\zeta,\tau)$ and those of the electric filed $\mathcal{E}(\zeta,\tau)$, for several times $\tau$, is reported in figure 1. The approach to the equilibrium configuration, both for the particle density (cfr. equation (3.11)) and the electric field (cfr. equation (3.12)), is clearly evident.

In figure 2, we report the theoretical spatial profiles of $\mathcal{N}(\zeta,\tau)$, at fixed time, for several values of the parameters $a$ and $b$. Large values of $a$ increase the adsorption capacity of the limiting surface, while large values of $b$ reduce the capability of desorption by the same limiting surface. Both effects translate into a major capability of this surface: capturing and maintaining particles. All of this is reflected in a larger shift of the actual particle density profile, at fixed time, from the initial configuration, $\mathcal{N}(\zeta,0)=1$, toward the equilibrium configuration, as clearly shown in the figure.

Finally, in figure 3 we depict the time evolution of the surface density of adsorbed particles $\mathcal{S}(\tau)$, for different values of the adsorption and desorption parameters.

## 4. Relaxation time

Let us suppose that for large $\tau$ the relaxation of the system toward the equilibrium is a simple process characterized by a relaxation time $\mathcal{T}$. In this case, we are entitled to seek a solution in the form

$$\mathcal{N}_{\mathrm{tr}}(\zeta,\tau)=\phi(\zeta)\,\mathrm{e}^{-\tau/\mathcal{T}}, \tag{4.1}$$

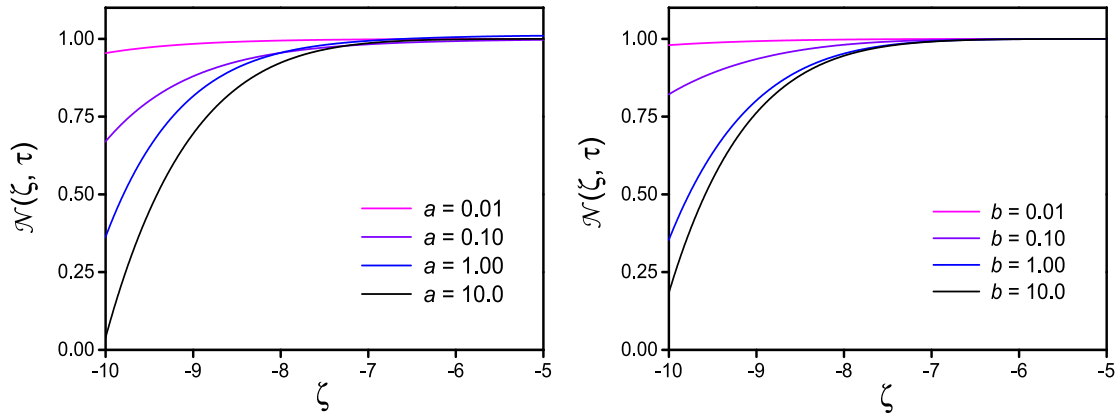


**Figure 2.** Theoretical spatial profiles of $\mathcal{N}(\zeta,\tau)$, at fixed time $\tau = 1$, for illustrative values of the parameters $a$ and $b$ for a cell with $M = 10$. Left panel: $b = 0.5$. Right panel: $a = 1$.

so that, from equation (3.14), we get

$$\phi(\zeta) = A_1\, \mathrm{e}^{\beta\zeta} + A_2\, \mathrm{e}^{-\beta\zeta}, \tag{4.2}$$

where

$$\beta = \sqrt{1 - \frac{1}{\mathcal{T}}}. \tag{4.3}$$

Accounting for the symmetry of the problem, we can write the solution in

$$\mathcal{N}_{\mathrm{tr}}(\zeta,\tau) = A\, \cosh\left(\beta\zeta\right) \mathrm{e}^{-\tau/\mathcal{T}}, \tag{4.4}$$

where $A$ is an integration constant, and consequently

$$\mathcal{E}_{\mathrm{tr}}(\zeta,\tau) = \frac{A}{\beta}\, \sinh\left(\beta\zeta\right) \mathrm{e}^{-\tau/\mathcal{T}}, \tag{4.5}$$

$$\mathcal{S}^{\mathrm{L/R}}_{\mathrm{tr}}(\tau) = \Gamma A\, \cosh\left(\beta M\right) \mathrm{e}^{-\tau/\mathcal{T}}, \tag{4.6}$$

where

$$\Gamma = a\, b\, \frac{\mathcal{T}}{\mathcal{T} - b}. \tag{4.7}$$

According to the boundary condition (2.9), from the above expressions, we obtain the relation

$$\tanh(\beta M) + \beta\Gamma = 0, \tag{4.8}$$

defining the relaxation time for the case under consideration. This relation, in the limit of $M \to \infty$, reduces to equation (57) of [5], valid when the sample is a half-space.

It is worth emphasizing the physical meaning of the limit $M \to \infty$. Since $M = d/(2\Lambda)$, increasing $M$ corresponds to increasing the plate separation relative to the Debye screening length. In this limit, $\tanh(\beta M) = 1$, so that equation (4.8) reduces to $1 + \beta\Gamma = 0$, which coincides with the characteristic equation previously obtained for the semi-infinite geometry (see equation (57) of [5]). Therefore, the longest relaxation time becomes independent of the sample thickness, indicating that the two interfaces are effectively decoupled. Physically, when $d \gg \Lambda$, the electric double layers localized near the electrodes do not overlap, and the finite-size corrections vanish as $M$ increases. Conversely, when the plate separation is only a few Debye lengths, the overlap of the diffuse layers produces a coupling between the two interfaces, making the relaxation dynamics dependent on the cell thickness. Consequently, the The finite-slab formulation is particularly relevant for nanometric confinement, whereas micrometer-thick cells, for which $M \gg 1$, are already well described by the semi-infinite approximation.

From equation (4.8) we can investigate the dependence of $\mathcal{T}$, related to the longest relaxation time, on the parameter $M$. Trivially, we have

$$M = -\frac{1}{\beta}\, \mathrm{arctanh}\left(\beta\Gamma\right), \tag{4.9}$$

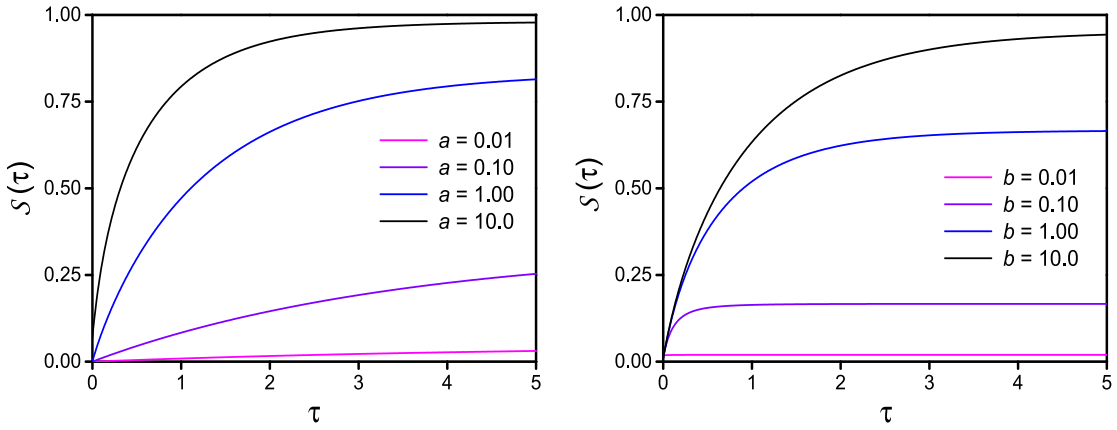


**Figure 3.** Time evolution of profiles of the surface density of adsorbed particles $\mathcal{S}(\tau)$, for illustrative values of the parameters $a$, $b$, and $M$ as reported in figure 2.

so that, for $\mathcal{T} > 1$, the quantity $M$ assume physical acceptable values only for $1 < \mathcal{T} < b$ and

$$a \leqslant \frac{1}{\beta}\left(\frac{1}{\mathcal{T}} - \frac{1}{b}\right), \tag{4.10}$$

diverging at the equality.

Otherwise, in the case where $0 < \mathcal{T} < 1$, solutions of the symmetric slab becomes

$$\mathcal{N}_{\rm tr}(\zeta,\tau) = A\cos\left(\beta\zeta\right)\mathrm{e}^{-\tau/\mathcal{T}}, \tag{4.11}$$

$$\mathcal{E}_{\rm tr}(\zeta,\tau) = \frac{A}{\beta}\sin\left(\beta\zeta\right)\mathrm{e}^{-\tau/\mathcal{T}}, \tag{4.12}$$

$$\mathcal{S}_{\rm tr}(\tau) = \Gamma A\cos\left(\beta M\right)\mathrm{e}^{-\tau/\mathcal{T}}. \tag{4.13}$$

Now, from the boundary condition (2.9), we get the compatibility equation

$$\tan\left(\beta M\right) + \beta\Gamma = 0, \tag{4.14}$$

which has infinite solutions. Consequently, we have infinite eigenfunctions by means of which we can satisfy the initial boundary condition, as discussed previously in [31].

## 5. External power supply

Until now, we have investigated the evolution of the system toward equilibrium when adsorption–desorption phenomena occur at the electrode surfaces. In this section, we explore the system evolution toward equilibrium, including the presence of an external power supply.

We assume the system initially in its own equilibrium under the sole adsorption effect, as described by equations (3.11)–(3.13). The present potential across the cell is

$$\mathcal{V}_{\rm eq}(\zeta) = ab\,\frac{\cosh(\zeta) - \cosh(M)}{\sinh(M) + ab\cosh(M)}, \tag{5.1}$$

where $\mathcal{V} = V/V_{\rm th}$ is the dimensionless electric potential measured in $V_{\rm th}$ units, and we fixed the gauge such that $\mathcal{V}_{\rm eq}(-M) = \mathcal{V}_{\rm eq}(M) = 0$. At $\tau = 0$ the external power supply is turned on, and the system evolves toward a new equilibrium configuration reached at $\tau \to \infty$.

During the transition, the electric potential profile across the cell, $\mathcal{V}(\zeta,\tau)$, may be separated in the transient and equilibrium components according to

$$\mathcal{V}(\zeta,\tau) = \mathcal{V}_{\rm eq}(\zeta) + \mathcal{V}_{\rm tr}(\zeta,\tau), \tag{5.2}$$

with the initial condition

$$\mathcal{V}(\zeta,0) = \mathcal{V}_{\rm eq}(\zeta) + \mathcal{V}_{\rm tr}(\zeta,0) = 0, \tag{5.3}$$

that is $\mathcal{V}_{\rm tr}(\zeta,0)=-\mathcal{V}_{\rm eq}(\zeta)$.

Actually, the presence of the external charge generator forces the potential at the surfaces to

$$\mathcal{V}(\zeta,\tau)\Big|_{\zeta=\mp M}=\mp\frac{\mathcal{V}_0}{2}f(\tau), \tag{5.4}$$

where $f(\tau)$ is a characteristic of the power supply, such that $f(\tau)=0$ for $\tau\leqslant 0$ and $f(\tau)=1$ in the $\tau\to\infty$ limit. As discussed in [31], a good approximation for $f(\tau)$ is

$$f(\tau)=1-\mathrm{e}^{-\tau/\mathcal{T}_{\rm R}}, \tag{5.5}$$

where $\mathcal{T}_{\rm R}$ is the rising time of the external power supply. Consequently, for $\tau\to\infty$, the transient components tend to zero, and the new equilibrium potential becomes

$$\widetilde{\mathcal{V}}_{\rm eq}(\zeta)\Big|_{\zeta=\mp M}=\mp\frac{\mathcal{V}_0}{2}, \tag{5.6}$$

while

$$\mathcal{V}_{\rm tr}(\zeta,\tau)\Big|_{\zeta=\mp M}=\pm\frac{\mathcal{V}_0}{2}\,\mathrm{e}^{-t/\mathcal{T}_{\rm R}}. \tag{5.7}$$

Therefore, the total electric potential at the electrodes is

$$\mathcal{V}(\zeta,\tau)\Big|_{\zeta=\mp M}=\mp\frac{\mathcal{V}_0}{2}\left(1-\mathrm{e}^{-\tau/\mathcal{T}_{\rm R}}\right), \tag{5.8}$$

and, as always, the electric potential is related to the electric field according to $\mathcal{E}=-\partial\mathcal{V}/\partial\zeta$.

In this framework, the fundamental equations governing the problem are again equations (2.4) and (2.5), hereinafter rewritten in

$$\frac{\partial\mathcal{N}}{\partial\tau}=\frac{\partial^2}{\partial\zeta^2}\left(\mathcal{N}+\mathcal{V}\right), \tag{5.9}$$

$$\frac{\partial^2\mathcal{V}}{\partial\zeta^2}=1-\mathcal{N}, \tag{5.10}$$

together with the kinetic equation (2.6), supplemented by the boundary conditions at the superficies (2.8).

To study the evolution of the system toward the new equilibrium configuration, hereinafter denoted in $\widetilde{\mathcal{N}}_{\rm eq}(\zeta)$, we again separate all relevant quantities into equilibrium and transient parts, i.e. $\mathcal{N}(\zeta,\tau)=\widetilde{\mathcal{N}}_{\rm eq}(\zeta)+\mathcal{N}_{\rm tr}(\zeta,\tau)$. Therefore, starting from the equilibrium under the sole effect of adsorption, $\mathcal{N}_{\rm eq}(\zeta)$ (cfr. equation (3.11)) the system evolves toward the new equilibrium configuration, $\widetilde{\mathcal{N}}_{\rm eq}(\zeta)$, fixed by the external potential.

The new equilibrium is a solution of the following equations:

$$\frac{\partial^2}{\partial\zeta^2}\left(\widetilde{\mathcal{N}}_{\rm eq}+\widetilde{\mathcal{V}}_{\rm eq}\right)=0, \tag{5.11}$$

$$\frac{\partial^2\widetilde{\mathcal{V}}_{\rm eq}}{\partial\zeta^2}=1-\widetilde{\mathcal{N}}_{\rm eq}, \tag{5.12}$$

together with the kinetic equations

$$\widetilde{\mathcal{S}}^{\rm L/R}_{\rm eq}(\zeta)=ab\widetilde{\mathcal{N}}_{\rm eq}(\zeta)\Big|_{\zeta=\mp M}, \tag{5.13}$$

and the boundary conditions at the surface

$$\frac{\partial}{\partial\zeta}\left(\widetilde{\mathcal{N}}_{\rm eq}(\zeta)+\widetilde{\mathcal{V}}_{\rm eq}(\zeta)\right)_{\zeta=\mp M}=0. \tag{5.14}$$

However, in the presence of an external potential, the Coulomb theorem at the adsorbing surfaces becomes

$$\mathcal{S}^{\rm L}(\tau)-\Sigma(\tau)=-\frac{\partial}{\partial\zeta}\mathcal{V}(\zeta,\tau)\Big|_{\zeta=-M}, \tag{5.15}$$

and

$$\mathcal{S}^{\mathrm{R}}(\tau)+\Sigma(\tau)=\frac{\partial}{\partial\zeta}\mathcal{V}(\zeta,\tau)\Big|_{\zeta=M}, \tag{5.16}$$

where the total surface density of electric charge came from the contribution of the adsorbing effect $\mathcal{S}^{\mathrm{L/R}}(\tau)$ and that of the generator, which accumulates the same but opposite charge quantity $\Sigma(\tau)$ on the two surfaces.

Note that, in the presence of an external power supply, the symmetry of the system is broken, so that the surface density of electric charge due to adsorption is different on the two surfaces, i.e. $\mathcal{S}^{\mathrm{L}}(\tau)\neq\mathcal{S}^{\mathrm{R}}(\tau)$.

Summing equations (5.15) and (5.16), and taking into account equation (5.13), we get the condition for the conservation of the number of particles

$$ab\left(\widetilde{\mathcal{N}}_{\mathrm{eq}}(-M)+\widetilde{\mathcal{N}}_{\mathrm{eq}}(M)\right)+\int_{-M}^{M}\left(\widetilde{\mathcal{N}}_{\mathrm{eq}}(\zeta)-1\right)\mathrm{d}\zeta=0, \tag{5.17}$$

that replaces equation (2.7) holding in the absence of an external power supply.

We get

$$\widetilde{\mathcal{N}}_{\mathrm{eq}}(\zeta)=1-\frac{ab\cosh(\zeta)}{\sinh(M)+ab\cosh(M)}-\frac{\mathcal{V}_0}{2}\frac{\sinh(\zeta)}{\sinh(M)}, \tag{5.18}$$

$$\widetilde{\mathcal{V}}_{\mathrm{eq}}(\zeta)=ab\frac{\cosh(\zeta)-\cosh(M)}{\sinh(M)+ab\cosh(M)}+\frac{\mathcal{V}_0}{2}\frac{\sinh(\zeta)}{\sinh(M)}, \tag{5.19}$$

$$\widetilde{\mathcal{S}}_{\mathrm{eq}}^{\mathrm{L/R}}=\frac{ab}{1+ab\coth(M)}\pm\frac{\mathcal{V}_0}{2}ab. \tag{5.20}$$

It is of some importance to note that the equilibrium profile for the electric potential relevant to the case of a semi-infinite sample cannot be deduced from (5.19) by performing the limit $M\to\infty$. In fact, for that situation in the limit of $\zeta\to\infty$, the potential has to tend to 0, whereas in the present case it tends to $\mathcal{V}_0/2$. From the expression of the electric potential at the limiting surfaces, it follows that the presence of the external power supply gives a total surface charge density

$$\Sigma_{\mathrm{eq}}=\frac{\mathcal{V}_0}{2}\left(\coth(M)+ab\right), \tag{5.21}$$

and, in the case of large $M$, the related surface field is $(\mathcal{V}_0/2)(1+ab)$.

Now, we look at the transient solutions in the presence of the external power supplies. We seek again for a solution to the system of partial differential equations

$$\frac{\partial\mathcal{N}_{\mathrm{tr}}}{\partial\tau}=\frac{\partial^2\mathcal{N}_{\mathrm{tr}}}{\partial\zeta^2}-\mathcal{N}_{\mathrm{tr}}, \tag{5.22}$$

and

$$\frac{\partial^2\mathcal{V}_{\mathrm{tr}}}{\partial\zeta^2}=-\mathcal{N}_{\mathrm{tr}}, \tag{5.23}$$

together with the kinetic equation

$$\mathcal{N}_{\mathrm{tr}}(\zeta,\tau)\Big|_{\zeta=\mp M}=\frac{1}{a}\left(\frac{\partial}{\partial\tau}+\frac{1}{b}\right)\mathcal{S}_{\mathrm{tr}}^{\mathrm{L/R}}(\tau), \tag{5.24}$$

and the boundary conditions at the sample surfaces

$$\frac{\mathrm{d}}{\mathrm{d}\tau}\mathcal{S}_{\mathrm{tr}}^{\mathrm{L/R}}(\tau)=\pm\frac{\partial}{\partial\zeta}\Big(\mathcal{N}_{\mathrm{tr}}(\zeta,\tau)+\mathcal{V}_{\mathrm{tr}}(\zeta,\tau)\Big)_{\zeta=\mp M}. \tag{5.25}$$

The initial conditions of the problem are

$$\mathcal{N}_{\mathrm{tr}}(\zeta,0)=\mathcal{N}_{\mathrm{eq}}(\zeta)-\widetilde{\mathcal{N}}_{\mathrm{eq}}(\zeta)=\frac{\mathcal{V}_0}{2}\frac{\sinh(\zeta)}{\sinh(M)}, \tag{5.26}$$

on the particle number and equation (5.7) on the electric potential.

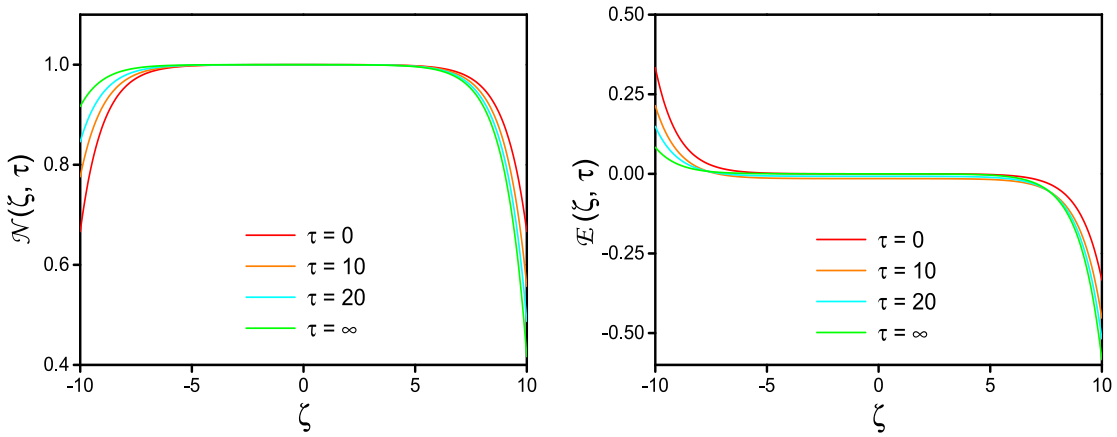


**Figure 4.** Left panel: shape of $\mathcal{N}(\zeta, \tau)$ vs $\zeta$, approaching the new equilibrium configuration (green line) (cfr. equation (5.18)), depicted for several values of $\tau$. The initial distribution (red line) corresponds to the starting equilibrium configuration given in equation (3.11). Right panel: shape of $\mathcal{E}(\zeta, \tau)$ vs $\zeta$, approaching the new equilibrium configuration (green line) (cfr. equation (5.19)), depicted for several values of $\tau$. The initial distribution (red line) corresponds to the starting equilibrium configuration given in equation (2.6). The curves are drawn for $a = 1$, $b = 0.5$, $M = 10$, $\mathcal{T}_{\rm R} = 2$ and $\mathcal{V}_0 = 0.5$.

The analytical solution of the whole problem is derived in appendix B and is summarized in

$$\mathcal{N}(\zeta,\tau) = 1 - \frac{a\,b\cosh(\zeta)}{\sinh(M) + a\,b\cosh(M)} - \frac{\mathcal{V}_0}{2}\frac{\sinh(\zeta)}{\sinh(M)} - \frac{\mathcal{V}_0}{2}\left(\frac{L(-1/\mathcal{T}_{\rm R})}{G(-1/\mathcal{T}_{\rm R})}\,{\rm e}^{-\tau/\mathcal{T}_{\rm R}} - \sum_{k=1}^{\infty}\frac{L(p_k)\,{\rm e}^{p_k\tau}}{p_k\,(1+\mathcal{T}_{\rm R}\,p_k)\,G'(p_k)}\right), \tag{5.27}$$

$$\mathcal{V}(\zeta,\tau) = a\,b\,\frac{\cosh(\zeta) - \cosh(M)}{\sinh(M) + a\,b\cosh(M)} + \frac{\mathcal{V}_0}{2}\frac{\sinh(\zeta)}{\sinh(M)} + \frac{\mathcal{V}_0}{2}\left(\frac{M(-1/\mathcal{T}_{\rm R})}{G(-1/\mathcal{T}_{\rm R})}\,{\rm e}^{-\tau/\mathcal{T}_{\rm R}} - \sum_{k=1}^{\infty}\frac{M(p_k)\,{\rm e}^{p_k\tau}}{p_k\,(1+\mathcal{T}_{\rm R}\,p_k)\,G'(p_k)}\right), \tag{5.28}$$

$$\mathcal{S}(\tau)^{\rm L/R} = \frac{a\,b}{1 + a\,b\coth(M)} \pm \frac{\mathcal{V}_0}{2}\,a\,b \mp \frac{\mathcal{V}_0}{2}\,a\,b\left(\frac{N(-1/\mathcal{T}_{\rm R})}{G(-1/\mathcal{T}_{\rm R})}\,{\rm e}^{-\tau/\mathcal{T}_{\rm R}} - \sum_{k=1}^{\infty}\frac{N(p_k)\,{\rm e}^{p_k\tau}}{p_k\,(1+\mathcal{T}_{\rm R}\,p_k)\,G'(p_k)}\right), \tag{5.29}$$

where

$$L(p) = -(1+p)\,(1+b\,p)\,\frac{\sinh\left(\zeta\sqrt{1+p}\right)}{\cosh\left(M\sqrt{1+p}\right)}, \tag{5.30}$$

$$M(p) = -\frac{(1+p)\,(1+b\,p)}{\cosh\left(M\sqrt{1+p}\right)}\left[\frac{\sinh\left(\zeta\sqrt{1+p}\right)}{1+p} + \zeta\,p\left(\frac{\cosh\left(M\sqrt{1+p}\right)}{\sqrt{1+p}} + a\,b\,\frac{\sinh\left(M\sqrt{1+p}\right)}{1+b\,p}\right)\right]. \tag{5.31}$$

$$N(p) = (1+p)\tanh\left(M\sqrt{1+p}\right). \tag{5.32}$$

The shape of the bulk density of particles $\mathcal{N}(\zeta, \tau)$ and those of the electric filed $\mathcal{E}(\zeta, \tau)$, for several time $\tau$ is reported in figure 4. The approach to the new equilibrium configuration, both for the particle density (cfr. equation (5.18)) and the electric field (cfr. equation (5.19)) is shown.

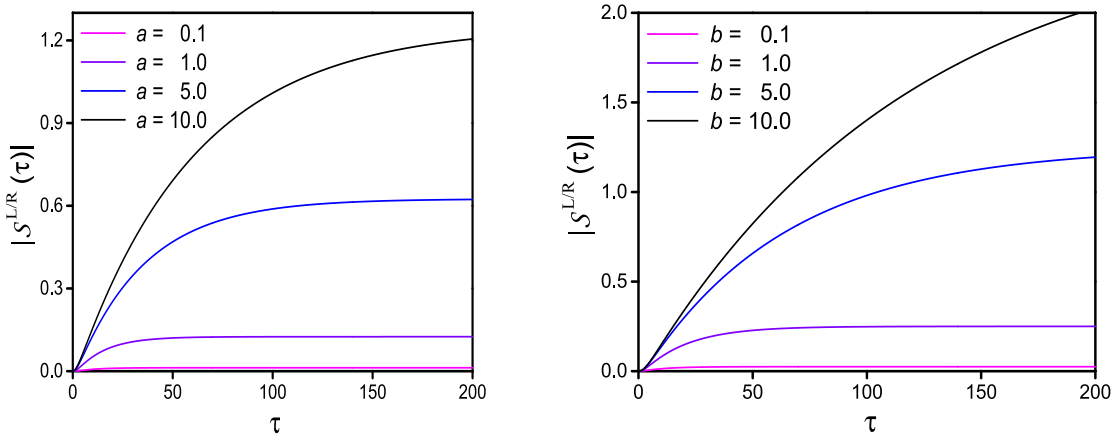


**Figure 5.** Time evolution of profiles of the absolute value of the transient surface density of adsorbed particles $|\mathcal{S}^{L/R}_{tr}(\tau)|$, for illustrative values of the parameters $a$ and $b$ for a cell with $M = 10$, $\mathcal{V}_0 = 0.5$ and $\mathcal{T}_R = 2$. Left panel: $b = 0.5$. Right panel: $a = 1$.

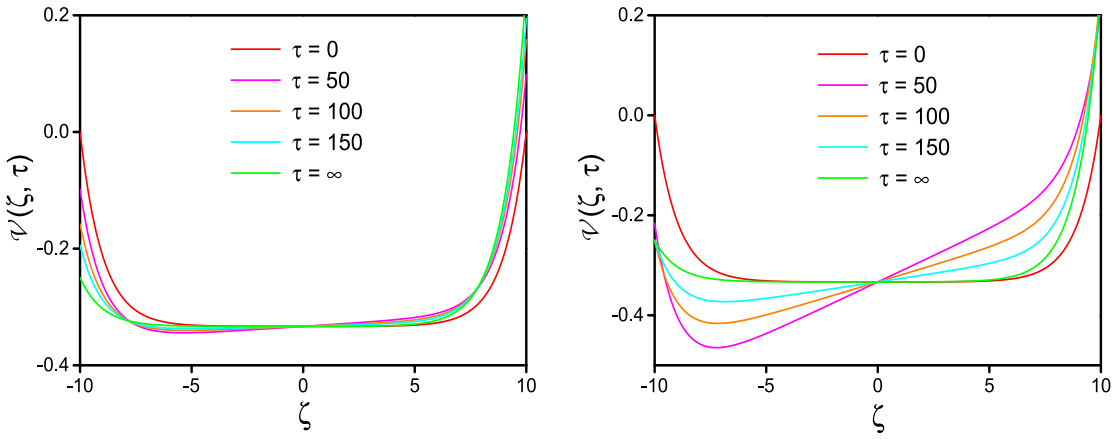


**Figure 6.** Comparison of the theoretical time evolution of the potential profiles $\mathcal{V}(\zeta, \tau)$ vs $\zeta$, for two different values of the rising time $\mathcal{T}_R$ of the external power supply. Left panel: $\mathcal{T}_R = 100$. Right panel: $\mathcal{T}_R = 0.5$. The curves are drawn for $a = 1$, $b = 0.5$, $M = 10$ and $\mathcal{V}_0 = 0.5$.

In figure 5, we depict the time evolution of the surface density of adsorbed particles $\mathcal{S}^{L/R}(\tau)$ referred to its initial equilibrium value given in equation (3.13). This correspond to the transient component $\mathcal{S}^{L}_{tr}(\tau) = -\mathcal{S}^{R}_{tr}(\tau)$. Therefore, the figure depict the shape of the absolute value of $\mathcal{S}^{L/R}_{tr}(\tau)$ for different values of the adsorption and desorption parameters.

The effects of the rising time of the external generator $\mathcal{T}_R$ on the evolution of the electric potential $\mathcal{V}(\zeta, \tau)$ inside the cell are well illustrated in figure 6. For a large value of the characteristic time (left panel), corresponding to a mild transition of the external potential to the boundary equilibrium condition (5.6), the electric potential within the cell gradually, with continuity, approaches the final equilibrium state (5.19). Differently, in the case of a small value of the characteristic time (right panel), corresponding to an abrupt transition of the external potential to the boundary equilibrium condition (5.6), the electric potential within the cell jumps to a large value, due to the perturbation generated by the external generator, and then approaches the equilibrium configuration from an unexpected direction.

## 6. Electric current

As discussed in [5], the total electric current density, given by the conduction current $j_{part}$ due to the contribution of the drift and the diffusion charge particles and the displacement current $j_{disp}$ due to the time variation of the electric field, is constant across the cell. This means that, also in the presence of an external power supply, the quantity

$$\mathcal{J}(\zeta, \tau) = j_{part}(\zeta, \tau) + j_{disp}(\zeta, \tau), \tag{6.1}$$

is, actually, a function only of time, i.e.

$$\frac{\partial \mathcal{J}}{\partial \zeta} = 0, \qquad \Rightarrow \qquad \mathcal{J} = \mathcal{J}(\tau), \tag{6.2}$$

where

$$j_{\rm part}(\zeta,\tau) = -\frac{\partial}{\partial \zeta}\Big(\mathcal{N}(\zeta,\tau) + \mathcal{V}(\zeta,\tau)\Big), \tag{6.3}$$

and

$$j_{\rm disp}(\zeta,\tau) = -\frac{\partial^2}{\partial \tau \partial \zeta}\mathcal{V}(\zeta,\tau). \tag{6.4}$$

At equilibrium, $j_{\rm part} = 0$ due to equation (5.14), while $j_{\rm disp} = 0$ since $\widetilde{\mathcal{V}}_{\rm eq}(\zeta)$ does not depend on $\tau$. Therefore, the total electric current density vanishes identically.

However, a transient current exists: $\mathcal{J}_{\rm tr} \neq 0$. From equation (6.1), we have

$$\mathcal{J}_{\rm tr}(\zeta,\tau)\Big|_{\zeta=\mp M} = -\frac{\partial}{\partial \zeta}\Big(\mathcal{N}_{\rm tr}(\zeta,\tau) + \mathcal{V}_{\rm tr}(\zeta,\tau) + \frac{\partial}{\partial \tau}\mathcal{V}_{\rm tr}(\zeta,\tau)\Big)_{\zeta=\mp M}, \tag{6.5}$$

where, according to the boundary condition (2.8) we can rewrite this relation in

$$\mathcal{J}_{\rm tr}(\zeta,\tau)\Big|_{\zeta=\mp M} = \mp\frac{\rm d}{{\rm d}\tau}\mathcal{S}_{\rm tr}^{\rm L/R}(\tau) - \frac{\partial^2}{\partial \zeta \partial \tau}\mathcal{V}_{\rm tr}(\zeta,\tau)\Big|_{\zeta=\mp M}. \tag{6.6}$$

By using equations (B.13)–(B.15) derived in appendix B, we get

$$\mathcal{J}_{\rm tr}(\zeta,\tau)\Big|_{\zeta=\mp M} = -\frac{\mathcal{V}_0}{2}\left(\frac{abN(-1/\mathcal{T}_{\rm R}) - M_\zeta(-1/\mathcal{T}_{\rm R})}{\mathcal{T}_{\rm R}\, G(-1/\mathcal{T}_{\rm R})}\,{\rm e}^{-\tau/\mathcal{T}_{\rm R}}\right.$$
$$\left. + \sum_{k=1}^{\infty}\frac{abN(p_k) - M_\zeta(p_k)}{(1+\mathcal{T}_{\rm R}p_k)\,G'(p_k)}\,{\rm e}^{p_k\tau}\right), \tag{6.7}$$

with

$$M_\zeta(p) = -(1+bp)\sqrt{(1+p)^3} - abp(1+p)\tanh\Big(M\sqrt{1+p}\Big).$$

Recalling equations (5.15) and (5.16), we get

$$\mathcal{J}_{\rm tr}(\zeta,\tau)\Big|_{\zeta=\mp M} = \frac{{\rm d}\Sigma}{{\rm d}\tau}, \tag{6.8}$$

that is the transient component of the total current across the cell. A simple integration gives

$$\Sigma = \frac{\mathcal{V}_0}{2}\Big(\coth(M) + ab\Big)$$
$$+ \frac{\mathcal{V}_0}{2}\left(\frac{abN(-1/\mathcal{T}_{\rm R}) - M_\zeta(-1/\mathcal{T}_{\rm R})}{G(-1/\mathcal{T}_{\rm R})}\,{\rm e}^{-\tau/\mathcal{T}_{\rm R}} - \sum_{k=1}^{\infty}\frac{abN(p_k) - M_\zeta(p_k)}{p_k(1+\mathcal{T}_{\rm R}p_k)\,G'(p_k)}\,{\rm e}^{p_k\tau}\right), \tag{6.9}$$

where, the integration constant has been fixed according to equation (5.21). To write an expression for the peak current as a function of the voltage rising time, we note that the transient current is given by a superposition of an infinite number of exponential modes. Therefore, the peak current is determined by the condition:

$$\frac{{\rm d}\mathcal{J}_{\rm tr}}{{\rm d}\tau} = 0, \tag{6.10}$$

which leads to a transcendental equation involving an infinite sum of exponentials. Consequently, neither the peak time nor the corresponding peak current can, in general, be expressed in closed analytical form, but can be obtained numerically.

## 7. Relaxation time with the external power supply

For the sake of simplicity, in this section, we pose $\mathcal{T}_{\rm R}=0$ corresponding to an abrupt increase of the potential at the surface from zero to $\mp\mathcal{V}_0/2$ and consequently the boundary condition on the transient component of the electric potential at the surfaces becomes

$$\mathcal{V}_{\rm tr}(\zeta,0)\Big|_{\zeta=\mp M}=0. \tag{7.1}$$

Even if this is a very ideal assumption, it does not invalidate the following analysis.

To start with, let us observe that the transient components of the dynamical functions characterizing the system must vanish at equilibrium. Since the governing equations are linear, the transient response can be expanded as a superposition of exponential eigenmodes. In the asymptotic limit ($\tau\to\infty$), all faster modes have decayed, and the dynamics are governed by the slowest eigenmode. The following analysis therefore focuses on the determination of this longest relaxation time. Therefore, we look for a solution of the type

$$\mathcal{N}_{\rm tr}(\zeta,\tau)=\phi(\zeta)\,{\rm e}^{-\tau/\mathcal{T}}, \tag{7.2}$$

$$\mathcal{V}_{\rm tr}(\zeta,\tau)=\chi(\zeta)\,{\rm e}^{-\tau/\mathcal{T}}, \tag{7.3}$$

that implies for the surface density of adsorbed particles, the time dependence

$$\mathcal{S}_{\rm tr}^{\rm L/R}(\tau)=\psi^{\rm L/R}\,{\rm e}^{-\tau/\mathcal{T}}. \tag{7.4}$$

A simple calculation [32] gives

$$\phi(\zeta)=A_1\,{\rm e}^{\beta\zeta}+A_2\,{\rm e}^{-\beta\zeta}, \tag{7.5}$$

$$\chi(\zeta)=-\frac{1}{\beta^2}\left(A_1\,{\rm e}^{\beta\zeta}+A_2\,{\rm e}^{-\beta\zeta}\right)+A_3\,\zeta+A_4, \tag{7.6}$$

where $A_i$, $i=1,2,3,4$, are integration constants to be determined by means of the boundary conditions (5.25) and (7.1).

Substituting the trial solutions (7.2) and (7.4) into (5.24) we get

$$\psi^{\rm L/R}=\Gamma\,\phi(\zeta)\big|_{\zeta=\mp M}, \tag{7.7}$$

where $\Gamma$ is defined in equation (4.7), while, the same substitution into (5.25), gives

$$\psi^{\rm L/R}=\mp\mathcal{T}\left(\phi'(\zeta)+\chi'(\zeta)\right)_{\zeta=\mp M}, \tag{7.8}$$

where prime denotes the derivative with respect to $\zeta$.

By comparing these last two relations, we get the compatibility conditions

$$\left(\pm\frac{\Gamma}{\mathcal{T}}\phi(\zeta)+\phi'(\zeta)+\chi'(\zeta)\right)_{\zeta=\mp M}=0. \tag{7.9}$$

Substituting (7.5) and (7.6) into (7.9) and accounting for the boundary condition on the potential (7.1), we get $A_i$ as a solution of the homogeneous system

$$\sum_{i=1}^{4}\mathcal{R}_{ij}A_j=0, \tag{7.10}$$

where $\mathcal{R}_{ij}$ are the entries of the matrix

$$\mathcal{R}=\begin{pmatrix} \left(\frac{\Gamma}{\mathcal{T}}+\beta-\frac{1}{\beta}\right){\rm e}^{-M\beta} & \left(\frac{\Gamma}{\mathcal{T}}-\beta+\frac{1}{\beta}\right){\rm e}^{M\beta} & 1 & 0\\ \left(-\frac{\Gamma}{\mathcal{T}}+\beta-\frac{1}{\beta}\right){\rm e}^{M\beta} & \left(-\frac{\Gamma}{\mathcal{T}}-\beta+\frac{1}{\beta}\right){\rm e}^{-M\beta} & 1 & 0\\ -\frac{1}{\beta^2}\,{\rm e}^{-M\beta} & -\frac{1}{\beta^2}\,{\rm e}^{M\beta} & -M & 1\\ -\frac{1}{\beta^2}\,{\rm e}^{M\beta} & -\frac{1}{\beta^2}\,{\rm e}^{-M\beta} & M & 1 \end{pmatrix}. \tag{7.11}$$

Since the system of linear equation (7.10) is homogeneous, a solution different from the trivial one, $A_i = 0$, exists only if

$$\mathrm{Det}[\mathcal{R}] = 0, \tag{7.12}$$

that defines the relaxation time of the system. This condition implies the following eigenvalue equation for the relaxation times

$$\frac{1}{\beta^3}\sinh^2(M\beta)\left(1+\Gamma\beta\coth(M\beta)\right)$$

$$\times\left(\mathcal{T}-\Gamma M\beta^2-M\beta\coth(M\beta)\right)=0, \tag{7.13}$$

that can be used to determine the longest relaxation time. It has to satisfy the conditions $\mathcal{T} > b > 1$, since only if the absorption is over the system can it reach the equilibrium state. In this case, $\Gamma > 0$, and, from equation (7.13), we conclude that the longest relaxation time follows from the relation

$$\mathcal{T} - M\beta\left(\Gamma\beta+\coth(M\beta)\right)=0. \tag{7.14}$$

In the cases of practical interest $\mathcal{T} \gg b$ and $M \gg 1$. In this situation, $\Gamma \approx ab$ so that, from equation (7.14), we get

$$\mathcal{T} = (1+ab)M. \tag{7.15}$$

For $a = 0$ we have $\mathcal{T} = M$, which coincides with the result reported in [26].

In the case of moderate $M$, expanding (7.14) in power series of $1/\mathcal{T}$, and than in power series of $1/M$, we get for the longest relaxation time the expression

$$\mathcal{T} = \frac{1}{2}\left[M(1+ab)+\sqrt{\Delta}\right], \tag{7.16}$$

where

$$\Delta = M[(1+ab)^2M+4a(b-1)b-2], \tag{7.17}$$

with $a$ and $b$ positive numbers in the range $.1-10$ (see [5]).

A simple numerical calculation shows that $\Delta > 0$ for all physically meaningful values of $a$ and $b$, if $M \geqslant 2$. This condition is fully consistent with the applicability of the continuum PNP description, since values ($M \lesssim 2$) correspond to sample thicknesses comparable to the Debye length, for which a continuum treatment of the ionic distribution becomes questionable. Consequently, equation (7.16) provides a real-valued approximation throughout the physically relevant parameter range considered in this work. However, the complete solution of the problem is a multi-relaxation phenomenon. Its solution can be obtained along the line discussed in [32].

Differently, in the absence of adsorption ($a = 0$, which implies $\Gamma = 0$), equation (7.13) simplifies in

$$\frac{1}{\beta^3}\sinh^2(M\beta)\left(\mathcal{T}-M\beta\coth(M\beta)\right)=0, \tag{7.18}$$

and the longest relaxation time follows trivially as a solution of the transcendental equation

$$\mathcal{T} = M\beta\coth(M\beta), \tag{7.19}$$

that coincides with that reported in [6].

## 8. Limits and merits of the proposed model

The objective of the present work is to obtain an analytical solution of the PNP model describing ionic relaxation in a slab geometry, accounting for both adsorption/desorption processes at the electrodes and the presence of an externally applied electric field. In order to achieve this goal, a number of simplifying assumptions have been introduced. Although these assumptions restrict the range of applicability of the model, they also make it possible to derive explicit analytical results that would otherwise be inaccessible. In this section, we briefly discuss these assumptions, their physical meaning, and possible directions for future extensions.

The first approximation consists of assuming that only one ionic species is mobile. Although in most liquid electrolytes both positive and negative ions contribute to charge transport, the single-mobile-ion approximation is well established for several experimentally relevant situations, such as polymer electrolytes and hydrogels containing fixed ionic groups, or systems in which one ionic species is effectively immobilized because of its large size or strong interaction with the surrounding matrix. The extension to the case in which both ionic species are mobile is, in principle, straightforward within the linear regime considered here, but leads to considerably more involved analytical calculations without modifying the qualitative physical picture.

A second assumption concerns the adsorption kinetics at the electrode surfaces. The adsorption equation employed in the analysis, equation (2.1), corresponds to the low-coverage limit of the Langmuir adsorption model. This approximation is valid provided that the surface coverage remains much smaller than the density of available adsorption sites, namely $\sigma \ll \sigma_{\max}$, where $\sigma_{\max}$ is typically of the order of $10^{18}$–$10^{19}$ sites on $m^2$ for solid surfaces. Under these conditions, the fraction of occupied sites is negligible, so that the nonlinear Langmuir factor $(1-\sigma/\sigma_{\max})$ can be approximated by unity.

Likewise, the present analysis assumes sufficiently small concentration perturbations and moderate applied voltages, so that steric crowding and finite-size effects remain negligible. At higher surface coverage or under stronger electric fields, nonlinear adsorption kinetics, finite-site saturation, Stern-layer corrections, and steric effects should be incorporated through more general models.

Another simplifying assumption is that ionic transport is governed exclusively by diffusion and electromigration. Convective transport and electroosmotic flow are neglected. This approximation is appropriate for quiescent systems, including solid electrolytes, polymer and ion-conducting gels with suppressed fluid motion, or liquid electrolytes in which externally driven convection and electroosmotic effects are negligible. In these situations, the standard PNP equations provide an adequate description of ionic transport. Incorporating electroosmotic flow would require coupling the PNP equations to the Navier–Stokes equations, considerably increasing the complexity of the problem.

Finally, the present model assumes independent Langmuir adsorption and a spatially uniform dielectric permittivity. Cooperative adsorption mechanisms, such as those described by Frumkin-type models, may become relevant when adsorbate–adsorbate interactions are significant. Likewise, the dielectric properties of the interfacial region may be modified by the presence of the adsorbed layer. Accounting for these effects would introduce additional interaction parameters and require a self-consistent treatment of a spatially varying dielectric response. While such extensions are certainly of physical interest, they lie beyond the scope of the present work [29, 33].

Despite these limitations, the proposed model provides an analytical description of ionic relaxation in finite electrolytic systems that incorporates both adsorption/desorption kinetics and externally applied electric fields. The resulting expressions for the transient concentration profiles, electric field, surface charge density, and relaxation times furnish a useful theoretical framework for interpreting experiments and constitute a convenient starting point for more comprehensive models including nonlinear adsorption, hydrodynamic effects, and more complex interfacial physics.

## 9. Concluding remarks

We have extended the theoretical analysis of the distribution of mobile charges in a semi-infinite medium bounded by a planar surface to the more realistic case of a finite slab, where two limiting surfaces can selectively adsorb positively charged particles. The interfacial dynamics have been assumed to follow Langmuir-type kinetics, with adsorption governed by the coefficient $\kappa_a$ and desorption characterized by the time $\tau_a$. The resulting accumulation of surface charge generates an electric field perpendicular to the interfaces, which significantly affects the bulk charge distribution.

The finite size of the system introduces a coupling between the two interfaces, leading to equilibrium and transient behaviors that differ markedly from the semi-infinite case. In particular, the spatial profiles

of the charge density and electric field, as well as the relaxation dynamics, are strongly influenced by the slab thickness and by the adsorption parameters.

The model has been solved analytically in the Laplace domain, allowing us to determine the full time evolution of the system. The corresponding time-dependent profiles have been obtained through a series expansion over the real poles of the Laplace-transformed solutions. Numerical evaluations have been presented for representative parameter regimes, illustrating the role of adsorption strength and system size.

The analytical expressions derived in the present work provide a theoretical framework for interpreting impedance spectroscopy measurements on finite electrolytic cells. In particular, they predict how the finite sample thickness and the adsorption/desorption kinetics modify the relaxation spectrum and the characteristic relaxation times. These predictions can be tested experimentally by varying the cell thickness or the interfacial adsorption properties.

The case in which the electrolytic cell is connected to an external power supply, as in real operating conditions, has also been analyzed. In this situation, the applied potential difference and the characteristic response time of the external circuit significantly affect the relaxation dynamics. In particular, the longest relaxation time depends sensitively on both the adsorption kinetics and the electrical driving conditions.

These results provide a comprehensive framework for describing charge redistribution in finite electrolytic systems with selective adsorption and may be relevant for the interpretation of impedance spectroscopy experiments and for the design of electrochemical devices.

## Acknowledgements

We are thankful to Ervin K. Lenzi for the useful discussion. L. R. E. gratefully acknowledges the hospitality of the Department of Molecular Sciences and Nanosystems at Ca' Foscari University of Venice, Italy, and the Department of Materials, Environmental Sciences and Urban Planning (SIMAU) at the Polytechnic University of Marche (UnivPM), Ancona, Italy, where he served as a Visiting Scholar during the preparation of this work.

## Data availability statement

All data that support the findings of this study are included within the article (and any supplementary files).

## Author contributions

A M Scarfone 0000-0001-6699-5889
Conceptualization (equal), Investigation (equal), Supervision (equal), Visualization (equal), Writing – original draft (equal), Writing – review & editing (equal)

G Barbero 0000-0002-2282-9536
Conceptualization (equal), Investigation (equal), Validation (equal), Writing – original draft (equal), Writing – review & editing (equal)

L R Evangelista 0000-0001-7202-1386
Conceptualization (equal), Investigation (equal), Validation (equal), Writing – original draft (equal), Writing – review & editing (equal)

## Appendix A. Analytical solution without external power supply

In this appendix, we seek a solution to the partial differential equation

$$\frac{\partial \mathcal{N}_{\rm tr}}{\partial \tau} = \frac{\partial^2 \mathcal{N}_{\rm tr}}{\partial \zeta^2} - \mathcal{N}_{\rm tr}, \tag{A.1}$$

constrained by the asymptotic condition $\mathcal{N}_{\rm tr}(\zeta,\infty)=0$, the initial condition

$$\mathcal{N}_{\rm tr}(\zeta,0)=1-\mathcal{N}_{\rm eq}(\zeta), \tag{A.2}$$

with $\mathcal{N}_{\rm eq}(\zeta)$ given in equation (3.11), and boundary conditions for the transient components

$$\mathcal{N}_{\rm tr}(0,\tau)=\mathcal{N}_{\rm tr}(2M,\tau)=\frac{1}{a}\frac{\partial}{\partial\tau}\mathcal{S}_{\rm tr}(\tau)+\frac{1}{ab}\mathcal{S}_{\rm tr}(\tau), \tag{A.3}$$

where

$$\mathcal{S}_{\rm tr}(\tau)=-\frac{1}{2}\int_{-M}^{M}\mathcal{N}_{\rm tr}(\zeta,\tau)\,{\rm d}\zeta=0. \tag{A.4}$$

The problem can be solved in the Laplace space by introducing the Laplace transform:

$$\mathcal{L}\left[\mathcal{N}_{\rm tr}\right](p)\equiv\Phi(\zeta,p)=\int_{0}^{\infty}\mathcal{N}_{\rm tr}(\zeta,\tau)\,{\rm e}^{-p\,\tau}\,{\rm d}\tau. \tag{A.5}$$

Equations equation (A.1), in terms of $\Phi(\zeta,p)$, becomes

$$\frac{\partial^2\Phi(\zeta,p)}{\partial\zeta^2}-(1+p)\,\Phi(\zeta,p)+\frac{ab\cosh(\zeta)}{\sinh(M)+ab\cosh(M)}=0, \tag{A.6}$$

where we used equation (A.2). Its solutions must satisfy equation (A.3), that in the Laplace space reads

$$\Phi(0,p)=\Phi(2M,p)=\frac{b}{1+ab\coth(M)}-\frac{1}{2ab}(1+bp)\int_{-M}^{M}\Phi(\zeta,p)\,{\rm d}\zeta. \tag{A.7}$$

The final solution is given by

$$\Phi(\zeta,p)=\frac{ab}{p}\frac{\cosh(\zeta)}{\sinh(M)+ab\cosh(M)}-ab\frac{\sqrt{1+p}}{p}\times\frac{\cosh\left(\zeta\sqrt{1+p}\right)}{ab\sqrt{1+p}\cosh\left(M\sqrt{1+p}\right)+(1+bp)\sinh\left(M\sqrt{1+p}\right)}. \tag{A.8}$$

In the limit of $M\to\infty$ from equation (A.8) we recover equation (A.8) of [5] for the semi-space, as expected.

We focus our attention now on the problem of finding the inverse Laplace transform of $\Phi(\zeta,p)$ that is, the particle number in the time domain. This task can be accomplished by means of the Fourier–Mellin integral [34, 35], that is

$$\mathcal{L}^{-1}\left[\Phi\right](\tau)\equiv\mathcal{N}_{\rm tr}(\zeta,\tau)=\frac{1}{2\pi i}\int_{\gamma-i\infty}^{\gamma+i\infty}\Phi(\zeta,p)\,{\rm e}^{p\,\tau}\,{\rm d}p, \tag{A.9}$$

respectively, where $\gamma=\Re(p)>\Sigma_p$ is the real part of $p$ and $\Sigma_p$ is the infimum of $p$ values for which the Laplace integral (A.5) converges.

Let us consider, firstly, the problem (A.9). To handle this integral, we rewrite it in

$$\mathcal{N}_{\rm tr}(\zeta,\tau)=\frac{1}{2\pi i}\int_{\ell}f(\zeta,p;\tau)\,dp, \tag{A.10}$$

where $f(\zeta,p;\tau)=\Phi(\zeta,p)\,{\rm e}^{p\,\tau}$ is a function defined in the complex plane of $p$ and $\ell$ is a contour in this complex plane including all the poles $p=p_k$ of $\Phi(\zeta,p)$ contributing to the integration in equation (A.10). According to the residue theorem, we have

$$\int_{\ell}f(\zeta,p;\tau)\,{\rm d}p=2\pi i\sum_{k=1}^{\infty}{\rm Res}f(\zeta,p_k;\tau). \tag{A.11}$$

It is easy to convince oneself that the pole at $p=0$ is actually a removable singularity since its residue is zero. Therefore we can rewrite the r.h.s. of (A.11) in a simplest manner

$${\rm Res}f(\zeta,p_k;\tau)=\frac{F(\zeta,p_k)}{G'(p_k)}\frac{{\rm e}^{p_k\,\tau}}{p_k\cosh\left(M\sqrt{1+p_k}\right)}, \tag{A.12}$$

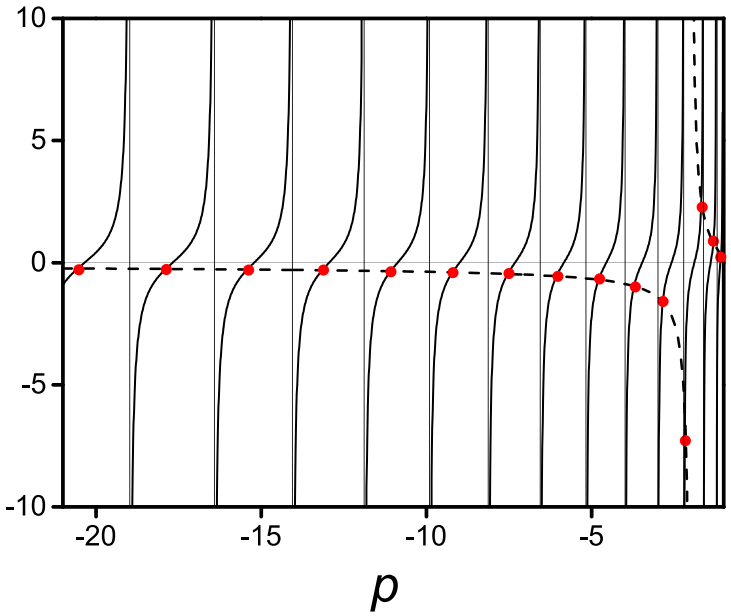


**Figure A1.** Locus poles (bullet), solution of equation (A.15), as intersection of the two curves $ab\sqrt{1+p}/(1+bp)$ (dash-line) and $-\tanh(M\sqrt{1+p})$ (full-line). The curves are drawn for $a=1$, $b=0.5$ and $M=10$.

where

$$F(\zeta,p)=-ab\sqrt{1+p}\cosh\left(\zeta\sqrt{1+p}\right), \tag{A.13}$$

and

$$G(p)=ab\sqrt{1+p}+(1+bp)\tanh\left(M\sqrt{1+p}\right), \tag{A.14}$$

are, respectively, the numerator and the denominator of the second factor in (A.8).

Therefore, the poles $p_k$ of $f(\zeta,p;\tau)$ follow from the condition $G(p_k)=0$, where $F(\zeta,p_k)\neq 0$, namely the algebraic solution of

$$ab\frac{\sqrt{1+p}}{1+bp}=-\tanh\left(M\sqrt{1+p}\right). \tag{A.15}$$

By inspection, it turns out that there are infinite roots of the equation (A.14), not equally spaced and all on the negative real axis of $p$, as shown in figure A1. The numerical values of the first few roots of equation (A.15) and the corresponding numerical coefficient of the residues, given in equation (A.12), are reported in table A1.

The final result can be written in

$$\mathcal{N}_{\rm tr}(\zeta,\tau)=-ab\sum_{k=1}^{\infty}\frac{\sqrt{1+p_k}\cosh\left(\zeta\sqrt{1+p_k}\right)}{G'(p_k)\,p_k\cosh\left(M\sqrt{1+p_k}\right)}\,{\rm e}^{p_k\tau}. \tag{A.16}$$

Consequently, from equations (3.8) and (3.10), we get the analytical expression of the transient component for the electric field

$$\mathcal{E}_{\rm tr}(\zeta,\tau)=ab\sum_{k=1}^{\infty}\frac{\sinh\left(\zeta\sqrt{1+p_k}\right)}{G'(p_k)\,p_k\cosh\left(M\sqrt{1+p_k}\right)}\,{\rm e}^{p_k\tau}, \tag{A.17}$$

and for the surface density of particles

$$\mathcal{S}_{\rm tr}(\tau)=ab\sum_{k=1}^{\infty}\frac{\tanh\left(M\sqrt{1+p_k}\right)}{G'(p_k)\,p_k}\,{\rm e}^{p_k\tau}. \tag{A.18}$$

**Table A1.** Position of the first fifteen poles of function $f(\zeta, p; \tau)$ of a system without external power supply (left column) and with external supply (right column) for $a = 1$, $b = 0.5$, and $M = 10$.

| | Poles ($\mathcal{V}_0 = 0$) | Poles ($\mathcal{V}_0 = 0.5$) |
|---|---|---|
| $p_1$ | −1.080 756 552 247 964 | −0.069 111 889 615 0980 |
| $p_2$ | −1.313 490 030 780 229 | −1.168 142 662 287 9785 |
| $p_3$ | −1.677 007 927 799 133 | −1.475 902 912 185 6694 |
| $p_4$ | −2.174 223 400 116 185 | −1.906 676 060 696 3083 |
| $p_5$ | −2.844 408 356 990 589 | −2.484 355 861 490 2120 |
| $p_6$ | −3.713 794 501 710 450 | −3.251 308 042 905 4063 |
| $p_7$ | −4.786 585 300 285 0502 | −4.222 098 568 500 7280 |
| $p_8$ | −6.061 160 697 352 605 | −5.396 161 127 864 4669 |
| $p_9$ | −7.535 883 718 249 179 | −6.771 273 144 005 2163 |
| $p_{10}$ | −9.209 721 168 832 516 | −8.345 963 800 115 8090 |
| $p_{11}$ | −11.082 059 197 750 258 | −10.119 389 891 793 341 |
| $p_{12}$ | −13.152 527 978 395 549 | −12.091 067 068 246 691 |
| $p_{13}$ | −15.420 897 586 255 366 | −14.260 707 544 495 969 |
| $p_{14}$ | −17.887 020 149 910 285 | −16.628 133 481 894 519 |
| $p_{15}$ | −20.550 797 484 483 453 | −19.193 230 793 110 376 |

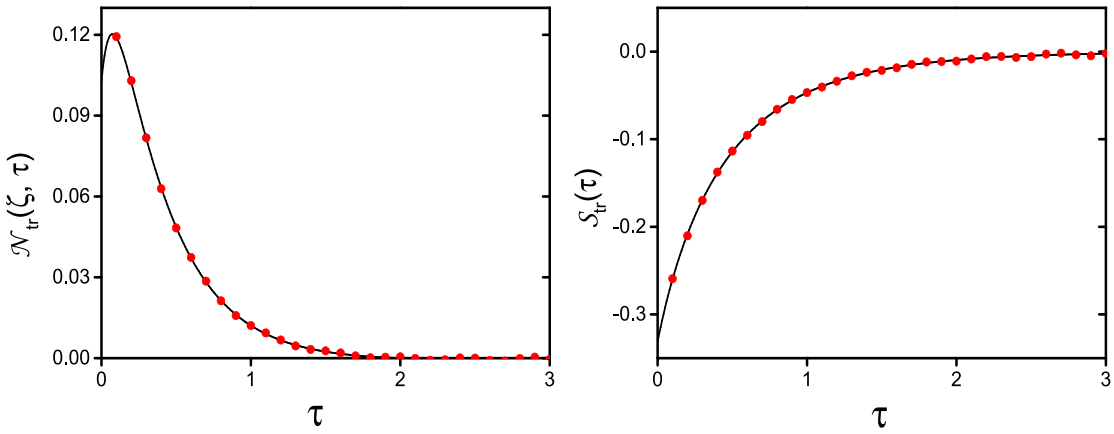


**Figure A2.** Left panel. Comparison of the analytical solution of $\mathcal{N}_{tr}(\zeta, \tau)$, given in equation (A.16) (full-line), and the numerical results of the inverse Laplace transform of $\Phi(p, \tau)$ given in equation (A.8) (dots), vs $\tau$ for $\zeta = 1$. Right panel. Comparison of the analytical solution of $\mathcal{S}_{tr}(\tau)$, given in equation (A.18) (full-line), and the numerical results of the inverse Laplace transform of $\Psi(\tau)$, given in equation (A.19) (dots), vs $\tau$. The curves are drawn for a system with $a = 1$, $b = 0.5$, and $M = 10$.

To show as this procedure works well, we compare in the left panel of figure A2 the analytical solution of $\mathcal{N}_{tr}(\zeta, \tau)$, given by equation (A.16) (full-line), with the numerical results of the inverse Laplace transform of $\Phi(p, \tau)$ given by equation (A.8) (dots), vs $\tau$ for $\zeta = 1$. In the right panel of the same figure, we compare the analytical solution of $\mathcal{S}_{tr}(\zeta, \tau)$, given by equation (A.18) (full-line), with numerical results of the inverse Laplace transform (dots) given by

$$\Psi(\tau) = -\frac{1}{2}\int_{-M}^{M} \Phi(\zeta, \tau)\, \mathrm{d}\zeta. \tag{A.19}$$

Although the analytical solutions are approximate for the first 15 residues, the agreement with the numerical results is remarkable.

Although the poles $p_k$ are obtained numerically as the roots of the transcendental equation (A.15), equations (A.16)–(A.18) constitute an analytical representation of the solution in the form of a residue expansion. Similar eigenvalue expansions are routinely encountered in classical boundary-value problems involving diffusion and heat conduction. Owing to the rapid decay of the exponential factors $e^{p_k \tau}$, only the first few poles are generally required to obtain accurate numerical results.

## Appendix B. Analytical solution with external power supply

Let us now look at the transient solutions of our problem in the presence of an external power supply. The main steps follow the same lines described above, that is, to seek a solution of equations (5.22)–(5.25) with the initial condition (5.7) for $\mathcal{V}_{\rm tr}(\zeta,\tau)$, (5.26) for $\mathcal{N}_{\rm tr}(\zeta,\tau)$ and $\mathcal{S}_{\rm tr}^{\rm L/R}(0)=\mp ab\mathcal{V}_0/2$.

Unlike the previous case, all the quantities to be determined are now entangled with one another. Therefore, we must translate the whole problem into the Laplace space by introducing, in addition to the Laplace transform of particles (A.5), also the Laplace transform of the electric potential

$$\mathcal{L}\left[\mathcal{V}_{\rm tr}\right](p)\equiv\chi(\zeta,p)=\int_0^\infty \mathcal{V}_{\rm tr}(\zeta,\tau)\,{\rm e}^{-p\tau}\,{\rm d}\tau, \tag{B.1}$$

and those of the adsorbed particle on the left and right plate

$$\mathcal{L}\left[\mathcal{S}_{\rm tr}^{\rm L/R}\right](p)\equiv\Psi^{\rm L/R}(\zeta,p)=\int_0^\infty \mathcal{S}_{\rm tr}^{\rm L/R}(\zeta,\tau)\,{\rm e}^{-p\tau}\,{\rm d}\tau. \tag{B.2}$$

In this way, the full problem to solve, accounting for the initial conditions, becomes

$$\frac{\partial^2\Phi(\zeta,p)}{\partial\zeta^2}-(1+p)\,\Phi(\zeta,p)+\frac{\mathcal{V}_0}{2}\,\frac{\sinh(\zeta)}{\sinh(M)}=0, \tag{B.3}$$

$$\frac{\partial^2\chi(\zeta,p)}{\partial\zeta^2}=-\Phi(\zeta,p), \tag{B.4}$$

$$\left(p+\frac{1}{b}\right)\Psi^{\rm L/R}(\tau)=a\,\Phi(\zeta,p)\Big|_{\zeta=0,\,2M}\mp a\,b\,\frac{\mathcal{V}_0}{2}, \tag{B.5}$$

$$\frac{\partial}{\partial\zeta}\Big[\Phi(\zeta,\tau)+\chi(\zeta,\tau)\Big]_{\zeta=\mp M}=\mp p\,\Psi^{\rm L/R}(p)-a\,b\,\frac{\mathcal{V}_0}{2}, \tag{B.6}$$

and the boundary condition on $\mathcal{V}_{\rm tr}(\zeta,p)$ given by

$$\mathcal{V}_{\rm tr}(\zeta,p)|_{\zeta=\mp M}=\pm\frac{\mathcal{V}_0}{2}\,\frac{1}{p+1/\mathcal{T}_{\rm R}}. \tag{B.7}$$

General solution of equations (B.3)–(B.5) reads

$$\Phi(\zeta,p)=\frac{\mathcal{V}_0}{2p}\left\{\frac{\sinh(\zeta)}{\sinh(M)}+c_1\sinh\left(\zeta\sqrt{1+p}\right)\right\}, \tag{B.8}$$

$$\chi(\zeta,p)=\frac{\mathcal{V}_0}{2p}\left\{\frac{\sinh(M-\zeta)}{\sinh(M)}+c_1\left[\frac{\sinh\left(\zeta\sqrt{1+p}\right)}{1+p}\right.\right.$$
$$\left.\left.+\zeta p\left(\frac{\cosh\left(M\sqrt{1+p}\right)}{\sqrt{1+p}}+a\,b\,\frac{\sinh\left(M\sqrt{1+p}\right)}{1+bp}\right)\right]\right\}, \tag{B.9}$$

$$\Psi^{\rm L/R}(\tau)=\mp a\,b\,\frac{\mathcal{V}_0}{2p}\left[1-\frac{c_1}{1+bp}\sinh\left(M\sqrt{1+p}\right)\right], \tag{B.10}$$

where the integration constant $c_1$ is fixed by consistency of equation (B.6). It is

$$c_1=\frac{(1+p)\,(1+bp)}{(1+p\,\mathcal{T}_{\rm R})\,G(p)}\,\mathrm{sech}\left(M\sqrt{1+p}\right), \tag{B.11}$$

with

$$G(p)=Mp\,(1+bp)\sqrt{1+p}$$
$$+\left[1+bp+ab\,Mp\,(1+p)\right]\tanh\left(M\sqrt{1+p}\right). \tag{B.12}$$

By using the residue theorem, solutions of the problem in the time-space can be obtained as an expansion around the poles of the transformed function. Let us observe that while the pole at $p=0$ is still

a removable singularity, there is a pole at $p=-1/\mathcal{T}_{\rm R}$ due to the transient of the external potential. Exceptionally, in the case of $\mathcal{T}_{\rm R}=1$, it disappears and does not contribute to the final solution,

$$\mathcal{N}(\zeta,\tau)=-\frac{\mathcal{V}_0}{2}\left(\frac{L(-1/\mathcal{T}_{\rm R})}{G(-1/\mathcal{T}_{\rm R})}\,{\rm e}^{-\tau/\mathcal{T}_{\rm R}}-\sum_{k=1}^{\infty}\frac{L(p_k)\,{\rm e}^{p_k\tau}}{p_k\,(1+\mathcal{T}_{\rm R}\,p_k)\,G'(p_k)}\right), \tag{B.13}$$

$$\mathcal{V}(\zeta,\tau)=\frac{\mathcal{V}_0}{2}\left(\frac{M(-1/\mathcal{T}_{\rm R})}{G(-1/\mathcal{T}_{\rm R})}\,{\rm e}^{-\tau/\mathcal{T}_{\rm R}}-\sum_{k=1}^{\infty}\frac{M(p_k)\,{\rm e}^{p_k\tau}}{p_k\,(1+\mathcal{T}_{\rm R}\,p_k)\,G'(p_k)}\right), \tag{B.14}$$

$$\mathcal{S}(\tau)^{\rm L/R}=\mp\frac{\mathcal{V}_0}{2}\,a\,b\left(\frac{N(-1/\mathcal{T}_{\rm R})}{G(-1/\mathcal{T}_{\rm R})}\,{\rm e}^{-\tau/\mathcal{T}_{\rm R}}-\sum_{k=1}^{\infty}\frac{N(p_k)\,{\rm e}^{p_k\tau}}{p_k\,(1+\mathcal{T}_{\rm R}\,p_k)\,G'(p_k)}\right]. \tag{B.15}$$

where

$$L(p)=-(1+p)\,(1+bp)\,\frac{\sinh\left(\zeta\sqrt{1+p}\right)}{\cosh\left(M\sqrt{1+p}\right)}, \tag{B.16}$$

$$M(p)=-\frac{(1+p)\,(1+bp)}{\cosh\left(M\sqrt{1+p}\right)}\left[\frac{\sinh\left(\zeta\sqrt{1+p}\right)}{1+p}+\zeta p\left(\frac{\cosh\left(M\sqrt{1+p}\right)}{\sqrt{1+p}}+a\,b\,\frac{\sinh\left(M\sqrt{1+p}\right)}{1+bp}\right)\right] \tag{B.17}$$

$$N(p)=(1+p)\,\tanh\left(M\sqrt{1+p}\right), \tag{B.18}$$

In equations (B.13)–(B.15), the first term is the residue at $p=-1/\mathcal{T}_{\rm R}$ and, as discussed above, it is not present in the special case of $\mathcal{T}_{\rm R}=1$.

## References


[1] Orazem M E and Tribollet B 2017 *Electrochemical Impedance Spectroscopy* (Wiley)
[2] Macdonald J R 1987 Impedance spectroscopy and its application to electrochemical systems *J. Electroanal. Chem.* **223** 25
[3] Barbero G, Evangelista L R, Lenzi E K and Scarfone A M 2024 Charge storage and potential difference generation in ion adsorbing cells *Eur. Phys. J. B* **97** 140
[4] Barbero G, Evangelista L R, Zola R S, Lenzi E K and Scarfone A M 2024 A brief review of fractional calculus as a tool for applications in physics: Adsorption phenomena and electrical impedance in complex fluids *Fractal Fract.* **8** 369
[5] Scarfone A M, Barbero G and Evangelista L R 2026 Electric field effects on the ionic relaxation in a semi-infinite adsorbing cell *J. Phys. A: Math. Theor.* **59** 205201
[6] Lelidis I, Alexe-Ionescu A L and Barbero G 2024 *J. Phys. Chem. C* **128** 949
[7] Newman J and Thomas-Alyea K E 2004 *Electrochemical Systems* 3rd edn (Wiley)
[8] Bard A J and Faulkner L R 2001 *Electrochemical Methods: Fundamentals and Applications* 2nd edn (Wiley)
[9] Bazant M Z, Kilic M S, Storey B D and Ajdari A 2009 Towards an understanding of induced-charge electrokinetics at large applied voltages in concentrated solutions *Adv. Colloid Interface Sci.* **152** 48
[10] Kilic M S, Bazant M Z and Ajdari A 2007 Steric effects in the dynamics of electrolytes at large applied voltages I. Double-layer charging *Phys. Rev. E* **75** 021502
[11] Kornyshev A A 2007 Double-layer in ionic liquids: paradigm change? *J. Phys. Chem. B* **111** 5545
[12] Bisquert J 2002 Theory of the impedance of electron diffusion and recombination in a thin layer *J. Phys. Chem. B* **106** 325–33
[13] Boukamp B A and Bouwmeester H J M 2003 *Interpretation of the Gerischer Impedance in Solid State Ionics* vol 157 (Solid State Ionics) pp 29–33
[14] Moya A A 2016 A ladder network modelling the electrochemical impedance of the diffusion and reaction processes in semi-infinite space *Phys. Chem. Chem. Phys.* **18** 3812–6
[15] Lelidis I and Barbero G 2017 Role of the displacement current on Warburg-type behavior *Phys. Rev. E* **95** 052604
[16] Ivan K, Kischner N, Simon P L, Jakab V, Merkin J H and Scott S K 2002 Direct evidence for fixed ionic groups in the hydrogel of an electrolyte diode *Phys. Chem. Chem. Phys.* **4** 1339
[17] Golovnev A and Trimper S 2009 Exact solution of the Poisson-Nernst-Planck equations in the linear regime *J. Chem. Phys.* **131** 114903
[18] Golovnev A and Trimper S 2011 Analytical solution of the Poisson-Nernst-Planck equations in the linear regime at an applied ac-voltage *J. Chem. Phys.* **134** 154902
[19] Gouy M 1910 Sur la constitution de la charge électrique à la surface d'un électrolyte *J. Phys. Theor. Appl.* **9** 457; Chapman D L 1913 A contribution to the theory of electrocapillarity *Philos. Mag.* **25** 475
[20] Delahay P 1965 Double layer and electrode kinetics, Interscience, New York
[21] Saifutdinov A I, Saifutdinova A A and Timerkaev B A 2018 Numerical study of the voltage waveform effect on the spatiotemporal characteristics of a dielectric barrier microdischarge in Argon *Plasma Phys. Rep.* **44** 359–68
[22] Yuchen H, Uehara S, Takana H and Nishiyama H 2016 Numerical modelling and simulation of chemical reactions in a nano-pulse discharged bubble for water treatment *Plasma Sci. Technol.* **18** 924

[23] Aleksandrov N L, Bazelyan E M, Ponomarev A A and Starikovsk A Y 2022 Kinetics of charged species in non-equilibrium plasma in water vapor- and hydrocarbon-containing gaseous mixtures *J. Appl. Phys.* **55** 383002
[24] Saifutdinov A I, Purin V V and Saifutdinova A A 2025 Towards a unified model of the low-current glow discharge with a liquid-phase anode *Plasma Phys. Rep.* **51** 1521–41
[25] Barbero G and Evangelista L R 2006 *Adsorption Phenomena and Anchoring Energy in Nematic Liquid Crystals* (Taylor and Francis)
[26] Bazant M, Thornton K and Ajdari A 2004 *Phys. Rev. E* **70** 021506
[27] Langmuir I 1916 The constitution and fundamental properties of solids and liquids *J. Am. Chem. Soc.* **38** 2221–95
[28] Bazant M, Storey B D and Kornyshev A A 2011 Double layer in ionic liquids: overscreening versus crowding *Phys. Rev. Lett.* **106** 046102
[29] Adamson A W and Gast A P 1997 *Physical Chemistry of Surfaces* 6th edn (Wiley)
[30] Probstein R F 2003 *Physicochemical Hydrodynamics: An Introduction* 2nd edn (Wiley)
[31] Scarfone A M, Aliyev Y and Barbero G 2025 Relaxation phenomenon in electrolytic cells limited by Ohmic electrodes *J. Phys. A: Math. Theor.* **58** 165204
[32] Barbero G, Aliyev Y and Scarfone A M 2024 Analytical description of the ionic relaxation in the presence of surface adsorption *J. Phys. A: Math. Theor.* **57** 265005
[33] Frumkin A N 1925 Electrocapillary curve of higher aliphatic acids and the state equation of the surface layer *Z. Phys. Chem.* **116** 466–70
[34] Kilbas A A, Srivastava H M and Trujillo J J 2006 *Theory and Applications of Fractional Differential Equations* (Elsevier)
[35] Evangelista L R and Lenzi E K 2023 *An Introduction to Anomalous Diffusion and Relaxation* (Springer)